ICE INITIATION BY AEROSOL PARTICLES: COMPARING MODEL PARAMETERIZATIONS AND OBSERVATIONS IN A PARCEL FRAMEWORK

T. Eidhammer[1], P. J. DeMott[1], D. C. Rogers[2], A. J. Prenni[1], M. D. Petters[1], C. H. Twohy[3], J. G. Hudson[4] and S. M. Kreidenweis[1]

[1]Department of Atmospheric Science, Colorado State University, Fort Collins, Colorado, USA
[2]National Center for Atmospheric Research, Boulder, Colorado, USA
[3]Department of Atmospheric and Oceanic Sciences, Oregon State University, Corvallis, OR, USA
[4]Atmospheric Science Division, Deserts Research Institute, Reno, NV, USA

1. INTRODUCTION

In parameterizing ice formation in numerical models, it is clearly desirable to account for the contributions of different aerosol types and their variable concentrations in the atmosphere. However, the link between aerosol and ice nucleation is still poorly understood. The ICE-L campaign (Ice in Cloud Experiment-Layer clouds) was designed to study the initiation of ice via heterogeneous nucleation in clouds by linking them to measurements of aerosol characteristics. The target was wave clouds, which offer the opportunity to separate heterogeneous ice nucleation from secondary ice formation processes. Airborne microphysical, thermodynamic and remote sensing measurements, in and around these clouds were conducted during ICE-L.

In idealized wave clouds, the air flow is laminar. Parcels follow the streamlines and spend only a few hundred seconds in the cloud. Thus precipitation and mixing are expected to be minimal. Parcel models are therefore suitable for modeling ice initiation in these clouds [*Cotton and Field*, 2002].

We have implemented three heterogeneous ice nucleation parameterizations that account for different aerosol types and concentrations into a Lagrangian parcel model. These parameterizations are tested for a selected case during ICE-L, and compared with the measurements.

2. PARCEL MODEL

The parcel model used in this study is an extended version of the Lagrangian parcel model developed by *Feingold and Heymsfield* [1992]. The original parcel model calculates droplet growth by condensation in an adiabatic updraft, or along trajectories, with prescribed atmospheric parameters. Some of the changes to the original parcel model are the inclusion of ice nucleation and crystal growth, and modification of the parameterization of water activity and hygroscopic growth for solution drops.

The calculation of water activity of a solution drop follows *Petters and Kreidenweis* [2007] where hygroscopicity is expressed with a single parameter κ. Kappa can be understood as the "unit volume of water that is associated with the unit volume of the dry aerosol" [*Petters and Kreidenweis*, 2007]. Further, internally mixed aerosols follow the simple mixing rule where κ is the sum of volume weighted κ_i of each individual component in the aerosol. Fairly complex aerosol types can therefore be assumed without having to determine the physiochemical properties, and the use of κ allows for straightforward implementation of internally, as well as externally mixed aerosols.

Three heterogeneous ice nucleation parameterizations developed by *Khvorostyanov and Curry* [2004], *Diehl and Wurzler* [2004] and *Phillips et al.* [2008] are implemented. The scheme by *Khvorostyanov and Curry* [2004], hereafter called KC04, is based on classical heterogeneous nucleation theory. Freezing rate is mainly dependent on temperature, water activity, and ice nuclei (IN) size and surface properties. The various aerosol types that can serve as IN are accounted for through the surface properties from choice of contact angle, relative area of

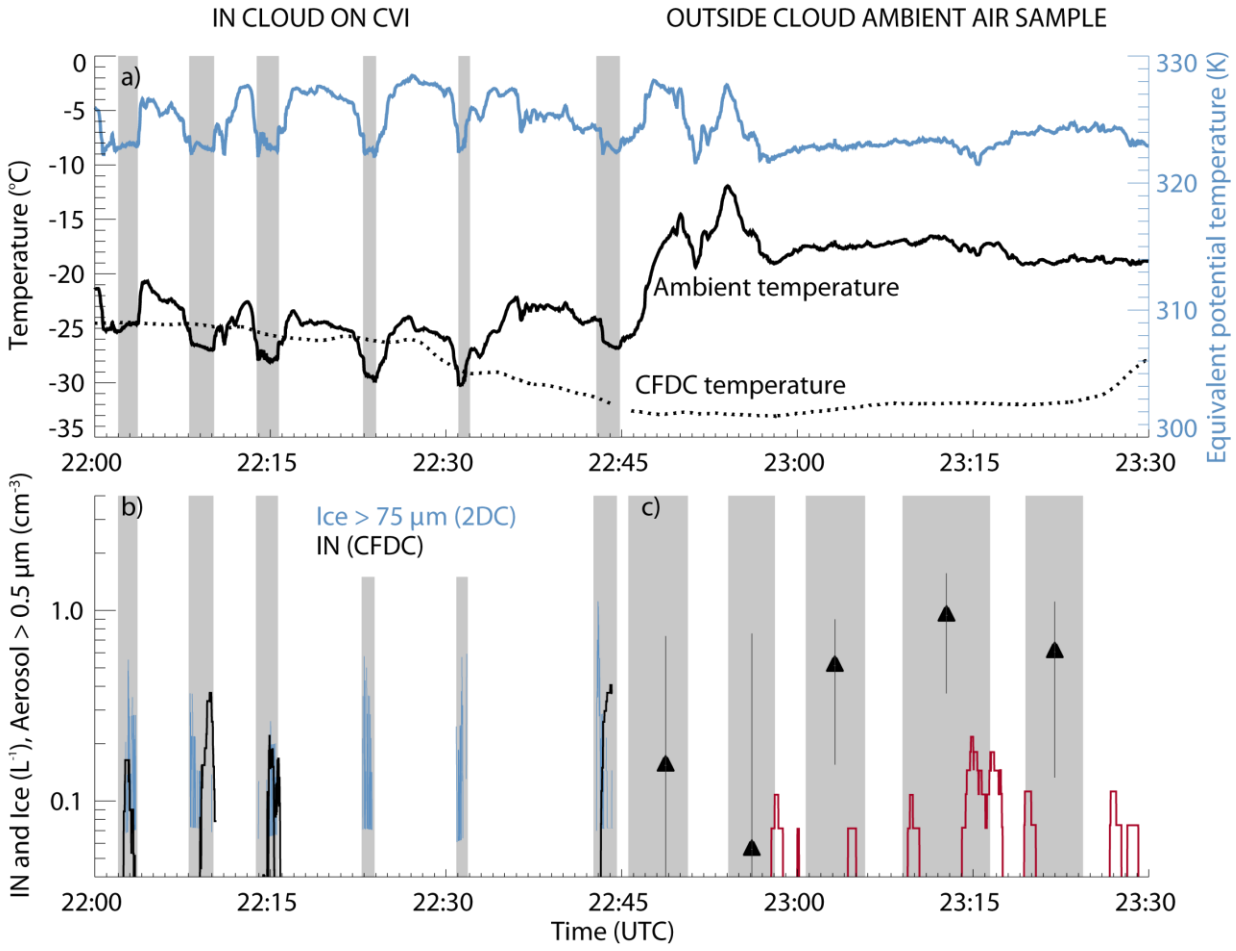

Figure 1 a) Ambient (black solid curve) and equivalent potential temperature (blue curve). Also shown are CFDC processing temperature (dotted curve). Grey areas indicate cloud passes. Note that a) spans over the entire time period. b) Ice > 75 µm (blue) and IN concentrations (black) in the cloud passes (up to about 22:45 UTC). The CFDC was on the CVI in this time period. c) Measured (triangles) interval-averaged IN concentrations from the ambient air sample inlet. The bars indicate the 90% confidence interval of the mean IN concentration. Grey areas here are measurement periods and white areas are CFDC filter periods. Also shown are aerosol concentration for particles > 0.5 µm in diameter (red lines).

active sites and misfit strain. The parameterization by *Diehl and Wurzler* [2004], hereafter called DW04, is based on laboratory measurements of freezing droplets, and include seven different aerosol types that can serve as IN (three types of mineral, three types of bacteria and soot). The freezing in this parameterization is mainly dependent on temperature and droplet volume. The *Phillips et al.* [2008] parameterization, hereafter called PDA08, is based on field measurements and constrained by laboratory measurements. Three different groups of aerosols are included (dust or metallic compounds, black carbon and insoluble organics). The number of IN from an aerosol population with these components is mainly related to the surface area of the aerosol population, temperature and saturation ratio.

While growth by droplets follow a Lagrangian framework in the parcel model, ice crystal growth follows a hybrid Eulerian/Lagrangian framework based on *Cooper et al.*, [1997].

3. CASE STUDY, NOVEMBER 18

3.1. Measurements

The NSF/NCAR C-130 aircraft served as the airborne measurement platform for ICE-L. Measurements were obtained over Colorado and Wyoming in November and December 2007. Due to the recent time frame of this experiment, all data used in this paper must be considered preliminary. We focus here on a wave-cloud mission on November 18. During this flight, two wave clouds were targeted. Here we consider the second cloud since aerosol measurements downwind of this cloud were obtained and can be used as initial conditions for the model.

In cloud

There were six passes through the cloud, at different altitudes. The passes were along, or in opposite direction to the horizontal component of the wind. Cloud level was between 7 and 7.5 km and temperatures were between -25 and -30°C as seen in Figure 1a, black solid curve. The grey shaded areas indicate the cloud passes. A clear sinusoidal wave structure, in some of the cloud passes, was evident from updrafts and temperature (not shown here) and vertical velocities in the wave were up to ± 3 m/s but with some variation in each pass.

Measured concentrations of ice > 75 µm and IN are shown in Figure 1b. The ice concentrations were measured with the NCAR "fast" 2DC probe which has a 64-diode array with 25 µm resolution and fast response electronics. The 2DC concentrations were between 0.05 and 0.6 L^{-1} for particles ≥ 75 µm (blue curve). IN measurements were conducted with an aircraft version of the Colorado State University Continuous Flow Diffusion Chamber (CFDC). This instrument is similar to the one described by *Rogers et al.* [2001], but with several modifications that will be described in a publication in preparation. Sample air within cloud was taken from a Counterflow Virtual Impactor (CVI) [*Twohy et al.*, 1997] and IN concentration was therefore only measured from cloud residual particles. The CFDC exposes sampled aerosols to a narrow range of processing temperature and relative humidity for a period of several seconds. Processing temperature was here close to the ambient temperature (dotted black curve in Figure 1a) and processing relative humidity ranged from 101 to 103% with respect to water to ensure that all aerosol particles are activated into cloud droplets, allowing them to freeze if an IN is present. The measurements indicate that 60 s average IN concentrations were up to 0.4 L^{-1} (black curve in Figure 1b). This is in agreement with the measured ice crystal concentration from the 2DC except for one cloud pass (22:23 UTC) where no IN were detected. This is expected due to the very low IN concentrations. No IN were measured during the 22:31 UTC cloud pass because the CDFC measured filtered air. There was a cloud layer above the target cloud, but University of Wyoming 85 Ghz cloudradar and lidar data indicate that the upper cloud maintained a separation of about 800 m (Zhien Wang, personal communication) and so there was probably no seeding of ice into the lower sampled cloud.

Cloud droplet concentrations (not shown here), which was measured with the Droplet Measurement Systems (Boulder, CO) Cloud Droplet Probe (CDP), were between 100 and 150 cm^{-3}.

Out of cloud

Aerosol measurements were obtained downwind of the cloud at the same equivalent potential temperature as in the cloud (~ 322 K, blue curve in Figure 1a).

In the region downwind of the cloud, IN measurements were conducted with an ambient air sample collected from an inlet that was separate from the CVI [*Rogers and DeMott*, 2002]. The inlet flow rate was adjusted to be isokinetic at the tip. The tip was heated to +7°C to avoid blocking from rime ice accumulating in regions of supercooled water. Measurement results are shown in Figure 1c. Here the grey areas indicate sampling periods while the white areas indicated filter periods to determine background counts in the CFDC method. Average IN concentrations are found for the intervals between the filter periods (triangles) and range from 0.05 to 1 L^{-1}. These concentrations compare well to the IN measurements in cloud. Error bars represent the 90% confidence interval of

mean IN concentration. Also shown are aerosol concentrations measured with a PMI Ultra-High Sensitivity Aerosol Spectrometer (UHSAS) of particles > 0.5 µm in diameter (red lines) since IN concentrations have shown positive correlations with aerosol concentrations in this size range [*Richardson et al.*, 2007].

3.2 Parcel Model Simulation

We performed a simple parcel modeling study, assuming a sinusoidal wave structure of ± 2.5 m/s. We used a combination of measurements of potential temperature and the vertical wind component to estimate the wavelength, which was about 2.7 km. With an average horizontal wind speed of 23 m/s, the wave parcel transit time is about 1100 s. The initial temperature is -23°C and initial relative humidity is 70%.

For aerosol input parameters, we used fitted size distributions from UHSAS measurements downwind of the cloud, where the equivalent potential temperature was 322 K. The aerosol measurements were obtained from 22:54 to 23:24 UTC. Since the initial aerosol distribution for the simulations is from downwind of the cloud, we assume that any potential cloud processing does not affect the aerosols. We performed simulations with an average input distribution form the entire period, and with four different input distributions, taken from the same time periods when the CFDC was sampling.

Three lognormal modes were fit to the 30 minute average distribution measured with UHSAS (Figure 2). The smallest mode is assumed to be ammonium sulfate and is allowed to act only as CCN, with κ_{as} = 0.6. The largest mode is assumed to be an internal mixture with 0.9 volume fraction dust (κ_d = 0.04) and 0.1 volume fraction ammonium sulfate (total κ_{d+as} = 0.9κ_d+0.1κ_{as}= 0.1). The second mode is assumed to not contribute to ice nucleation, and due to the low concentration compared to the first mode, for simplicity, this mode is not included in the simulations. Thus, only the largest mode contributes to ice crystal generation.

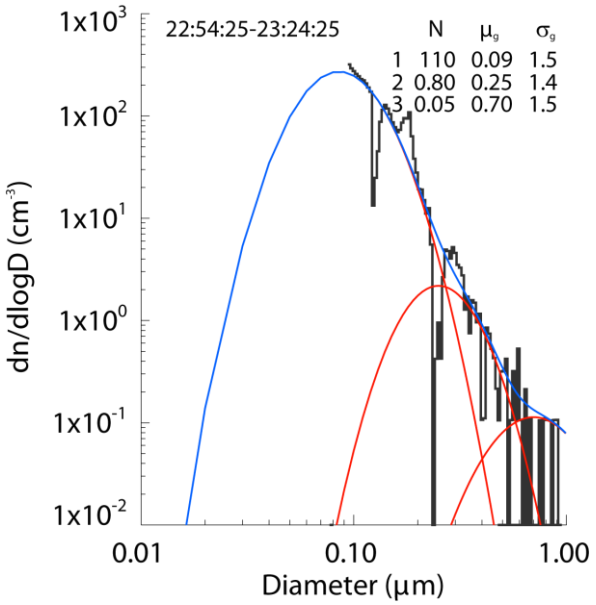

Figure 2 Measured 30 min average aerosol distributions (black lines) and fitted size distributions for the time period 22:54:25 – 23:24:25 UTC. Individual distributions are shown in red and total distribution is shown in blue.

Clearly the measured concentration of coarser mode particles is low, and the uncertainties of the fitted distributions are large. Further, the sizes measured with UHSAS are limited to > 0.1 µm and information of the distribution for smaller particles is not available at present. However, the integrated size distributions are comparable with measured CN concentrations.

For heterogeneous ice nucleation we used the three above-mentioned parameterizations.

3.3 Results

Figure 3 shows modeled ice concentrations using the average aerosol size distribution from the time period 22:54:25-23:24:25 UTC. Also shown are average ice crystal diameter, cloud droplet concentration, temperature, updraft and supersaturation. Different line styles represent different heterogeneous ice nucleation parameterizations. The solid line is the result using the PDA08 parameterization, and the ice crystal concentration is predicted to be about 0.9 L^{-1}, which is in reasonable agreement with measured IN con-

centrations (see Figure 1). All aerosols > 20 nm in the distribution activate cloud droplets and the modeled cloud droplet concentration is ~ 110 cm^{-3}. This compares well with measured cloud droplet concentration with the CDP (between 100 and 150 cm^{-3}). Further, CCN measurements were conducted with a DRI CCN spectrometer [*Hudson*, 1989]. Measurements in the ambient sampling region indicate an average CCN concentration of 70 cm^{-3} at supersaturation s = 0.5% and about 100 cm^{-3} at s = 1.05 %. The maximum supersaturation modeled in the parcel was 1.68%. This indicates that the assumption that all aerosols from the aerosol population can serve as CCN is adequate to model the droplet activation. Model temperatures range from -23 to -30°C and are in agreement with measurements. The droplets evaporate immediately (< 1 s) after reaching a relative humidity of 98%. The ice crystals, however, are too large to completely evaporate in the wave valley when relative humidity with respect to ice is less than 100%. Nevertheless, the simulated mean ice crystal diameter (~140 μm) is in reasonable agreement with 2DC ice crystal diameters that had a mode size near 180 μm.

The dotted lines in Figure 3 represent the DW04 parameterization. We assumed that the large particles are montmorillonite, which is one of the mineral types that can serve as IN in the DW04 parameterization. The predicted ice crystal concentration is close to 30 L^{-1}, which is in poor agreement with measurement. However, the droplet concentration is the same as measured and predicted with the Phillips parameterization.

The dashed lines represent the KC04 scheme. For this simulation we assumed that the contact angle was 50° (typical for quartz). All dust particles contribute to the modeled ice crystals with this parameterization. Since the ice crystal concentration is high, the ice crystal grows on expense of the droplets (Bergeron-Findeisen process), and water subsaturation is reached in the updraft. The droplets evaporate earlier than with the other parameterizations, and the mixed phased part of the cloud is therefore slightly smaller. To assume that all dust particles have the same contact angle, however, is probably not realistic. For example, freezing measurements of emulsified aqueous suspensions of dust can be modeled with

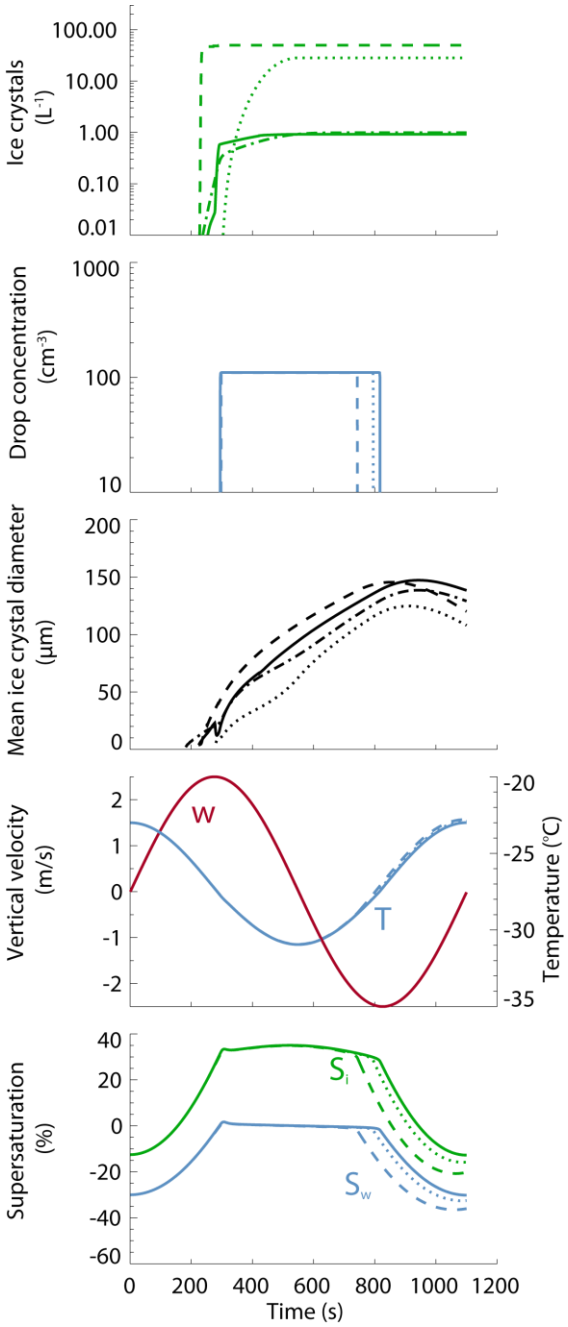

Figure 3 Modeled ice crystal and droplet concentrations in an idealized wave cloud. Also included are mean ice crystal diameter, temperature, updraft, and water and ice supersaturations along the trajectories. The different line styles are represented as follow: PDA08, solid curves; DW04, dotted curves; KC04, dashed curves; KC04 with contact angle probability function, dot dashed curves.

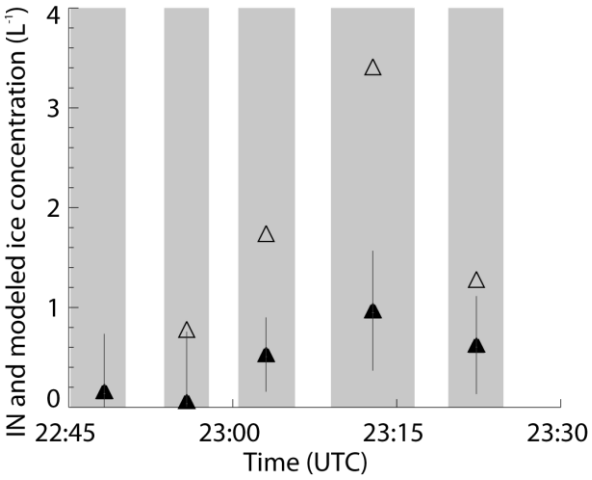

Figure 4 Modeled ice concentrations using the PDA08 parameterization (open triangles). Fitted size distributions from the same time periods as CFDC sampling periods (grey shaded areas) are used as initial size distributions for the simulations. Filled triangles are measured IN concentrations and are the same as in Figure 1c.

classical ice nucleation theory when assuming that each individual dust particle has a distribution of contact angles [*Marcolli et al.*, 2007]. If we assume that dust in each size class in our model has a contact angle distribution of

$$P(\theta) = 2 \cdot N(\mu,\sigma),$$

where N is the normal distribution, $\mu = 180^{\circ}$, $\sigma = 37$ and $0^{\circ} < \theta < 180^{\circ}$, then an ice crystal concentration of about 1 L^{-1} can be obtained with the KC04 parameterization (dot dashed curve in Figure 3). Note that this probability function is not based on measurements, but was constructed to reduce the freezing rate so KC04 model results could be reasonably comparable with measurements.

4. DISCUSSION AND CONCLUSION

The modeled ice crystal concentrations with the individual four size distributions from CFDC sampling period (measured size distributions not shown here), using the PDA08 parameterization are shown in Figure 4 as open triangles. Filled triangles are the measured IN concentrations from the same time period (also as shown in Figure 1c). All simulations are with same prescribed updrafts and temperatures as for Figure 3. The individual modeled ice crystal concentrations are up to a factor of 3.5 larger than the measured IN concentrations. The concentration of coarse mode aerosols was low, and the statistics in the individual size distributions have relatively larger uncertainties than the average distribution. Thus there are also larger uncertainties in the fitted individual distributions. However, the modeled ice crystal concentrations for each sample period follow the trend as seen for measured IN; higher concentration of aerosols above 0.5 µm relates to higher concentrations of IN (shown in Figure 1c).

We acknowledge that the thermodynamic path of particles through activation is different in the CFDC (rapid cooling from aircraft cabin temperature to a steady-state supercooled temperature and water supersaturation) compared to the wave cloud simulation, so a direct comparison between measured IN concentration and simulated ice crystal concentration must be viewed critically. However, both measurements and simulations reflect ice activation at similar peak water supersaturation conditions and comparable temperatures, Thus it is expected that the modeled ice crystal concentration should be in reasonable agreement with the measurements if the connection between aerosol properties and IN activation is specified correctly.

The PDA08 parameterization seems to predict ice crystal concentrations in closest agreement with IN measurements compared to the two other parameterizations considered. On the other hand, by assuming a contact angle distribution, the KC04 scheme can also predict ice crystal concentrations comparable with measurements. However, more information supporting typical contact angle distributions for dust are needed from many more atmospheric cases in varied regions.

For future work we plan to look at more cases from ICE-L along with cases from Wave-Ice [*Rogers and DeMott*, 2002]. Further, with more detailed information about the particle composition measured during ICE-L, additional aerosol types that can

serve as IN can be included in the model, such as carbonaceous and biologically derived particles. For now, only dust particles were assumed. However, the predicted ice crystal concentration with PDA08 scheme compares reasonably well with measurements by assuming that only dust particles are ice nuclei. Further, we also plan to constrain the simulations by using a combination of CCN data and composition from single particle aerosol mass spectrometry for the composition and mixing state of CCN.

5. BIBLIOGRAPHY

Cooper, W.A., R.T. Bruintjes, and G.K. Mather (1997), Calculations pertaining to hygroscopic seeding with flares, *J. Appl. Meteorol.*, *36*, 1449-1469

Cotton, R.J., and P.R. Field (2002), Ice nucleation characteristics of an isolated wave cloud, *Q. J. Royal Met. Soc.*, *128*, 2417-2437

Diehl, K., and S. Wurzler (2004), Heterogeneous drop freezing in the immersion mode: Model calculations considering soluble and insoluble particles in the drops, *J. Atmos. Sci.*, *61*, 2063-2072

Feingold, G., and A.J. Heymsfield (1992), Parameterizations of Condensational Growth of Droplets for Use in General-Circulation Models, *J. Atmos. Sci.*, *49*, 2325-2342

Hudson, J.G. (1989), An Instantaneous CCN Spectrometer, *J. Atmos. Ocean. Tech.*, *6*, 1055-1065

Khvorostyanov, V.I., and J.A. Curry (2004), The theory of ice nucleation by heterogeneous freezing of deliquescent mixed CCN. Part I: Critical radius, energy, and nucleation rate, *J. Atmos. Sci.*, *61*, 2676-2691

Marcolli, C., S. Gedamke, T. Peter, and B. Zobrist (2007), Efficiency of immersion mode ice nucleation on surrogates of mineral dust, *Atmos. Chem. Phys.*, *7*, 5081-5091

Petters, M.D., and S.M. Kreidenweis (2007), A single parameter representation of hygroscopic growth and cloud condensation nucleus activity, *Atmos. Chem. Phys.*, *7*, 1961-1971

Phillips, V.T.J., P.J. DeMott, and C. Andronache (2008), An empirical parameterization of heterogeneous ice nucleation for multiple chemical species of aerosol, *J. Atmos. Science*, *In press*

Richardson, M.S., P.J. DeMott, S.M. Kreidenweis, D.J. Cziczo, E.J. Dunlea, J.L. Jimenez, D.S. Thomson, L.L. Ashbaugh, R.D. Borys, D.L. Westphal, G.S. Casuccio, and T.L. Lersch (2007), Measurements of heterogeneous ice nuclei in the western United States in springtime and their relation to aerosol characteristics, *J. Geophys. Res*, *112*, D02209 doi:10.1029/2006JD007500

Rogers, D.C., and P.J. DeMott (2002), Ice crystal formation in wave clouds, airborn studies -10 to -35˚C., in *American Meterological Society Conference on Cloud Physics*, Ogden, UT

Rogers, D.C., P.J. DeMott, S.M. Kreidenweis, and Y.L. Chen (2001), A continuous-flow diffusion chamber for airborne measurements of ice nuclei, *J. Atmos. Ocean. Tech.*, *18*, 725-741

Twohy, C.H., A.J. Schanot, and W.A. Cooper (1997), Measurement of condensed water content in liquid and ice clouds using an airborne counterflow virtual impactor, *J. Atmos. Ocean. Tech.*, *14*, 197-202

6. ACKNOWLEDGEMENTS

This work has been supported by the National Science Foundation (NSF) Science and Technology Center for Multi-Scale Modeling of Atmospheric Processes, managed by Colorado State University under cooperative agreement No. ATM-0425247, NSF grant ATM-0611936, and by the NASA MAP (Modeling and Analysis Program) No. NNG06GB60G.